Investigations of the Chemical Potentials of Dissolved Water and H2S in CO2 Streams Using Molecular Dynamics Simulations and the Gibbs–Duhem Relation

ARTICLE *in* JOURNAL OF CHEMICAL & ENGINEERING DATA · SEPTEMBER 2015

Impact Factor: 2.04 · DOI: 10.1021/acs.jced.5b00267

4 AUTHORS, INCLUDING:

Bjørn Kvamme

University of Bergen

365 PUBLICATIONS **1,654** CITATIONS

SEE PROFILE

Sigvat Kuekiatngam Stensholt

Polytec

5 PUBLICATIONS **10** CITATIONS

SEE PROFILE

Journal of chemical & engineering data

Article

pubs.acs.org/jced

Investigations of the Chemical Potentials of Dissolved Water and H_2S in CO_2 Streams Using Molecular Dynamics Simulations and the Gibbs−Duhem Relation

Bjørn Kvamme,*[,†] Tatiana Kuznetsova,[†] Sigvat Stensholt,[‡] and Sara Sjöblom[†]

[†]Department of Physics, University of Bergen, 5020 Bergen, Norway

[‡]Polytec Research Foundation, Sørhauggata 128, 5527 Haugesund, Norway

ABSTRACT: Water that accompanies CO_2 during its pipeline transport presents a hazard due to rust and clathrate formation. Rusty pipeline walls favors adsorption of water and other impurities as an additional aqueous phase over condensing out as liquid droplets. The Gibbs phase rule prohibits the system from reaching full equilibrium since the continuous flow provides an ongoing supply of all phases. We present a scheme for free energy minimization under constraints of mass and heat transport that can predict the phase distribution and corresponding compositions. Molecular dynamics simulations and the Gibbs−Duhem relation are used to derive consistent infinite dilution chemical potentials for CO_2 and H_2S dissolved in water and H_2O and H_2S dissolved in CO_2. Simplified activity coefficient expressions are derived and applied to analysis of hydrate risk formation. Applications of our approach are illustrated by estimating the tolerable water concentration in CO_2 before water forms hydrate directly or adsorbs onto the rust. This limit is substantially lower for adsorption onto rust as opposed to condensing out. Investigating the water behavior as a solute in CO_2 highlights the question of whether it is thermodynamically feasible for water to dissolve as monomers or if it can thermodynamically benefit from forming dimers or clusters.

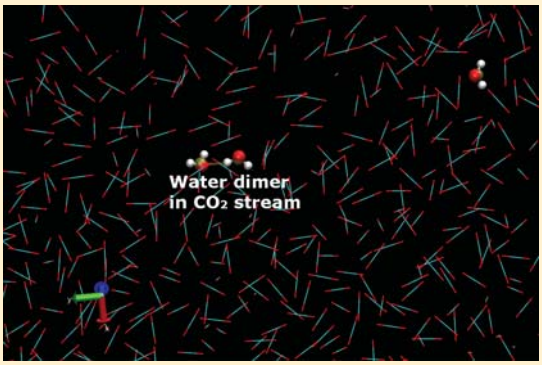

Publication Date (Web): September 9, 2015 | doi: 10.1021/acs.jced.5b00267

1. INTRODUCTION

Carbon dioxide underground sequestration projects underway in a number of countries call for large volumes of carbon dioxide (CO_2) to be transported via pipelines. CO_2 will be typically extracted from flue gas and contain a number of impurities. This work focuses on the presence of water and hydrogen sulfide (H_2S), both polar molecules with low solubility in other gases in general, including CO_2.

Given the conditions of seafloor transport, both of those impurities will create a number of possible challenges on the industrial level. In order to transfer sufficient quantities of CO_2, the gas must be under high pressure. Combined with the low temperature of ambient surroundings, this can lead to a very real risk of clathrate hydrates forming in the pipeline if the concentration of water is too high. Left unchecked, the solid crystalline structure of hydrates can cause blockage of pipeline and significant flow problems. The presence of H_2S, a notoriously aggressive hydrate former and corroder, can cause serious damage to industrial equipment.

Condensation which results in a free water phase can take place when this phase transition is thermodynamically favorable. For the given local temperature, this occurs if the dew-point pressure for the mixture is lower than the local pressure. In a system containing water, CO_2, H_2S, and some additional supercritical gases, the dew point will be totally dominated by water. A simplified approximated evaluation will therefore require evaluating the chemical potential of water dissolved in CO_2 and finding the pressure where this value is equal to that of liquid water under the same conditions. To determine whether condensation can occur, we need a means to compare the chemical potentials of all components in the different systems. Chemical potentials cannot be measured directly, although they can be derived from calorimetric studies using elementary relationships between free energy and enthalpy. From the thermodynamic viewpoint, it would be possible for hydrates to form homogeneously from water dissolved in CO_2[1] even though mass- and heat transport limitations will make this situation less likely.

A free water phase—either deposited as liquid droplets distributed inside the CO_2 phase or as a film of water on the pipeline walls—will give rise to a very favored heterogeneous hydrate formation on the water/CO_2 interface.

In a nonequilibrium system, the direction of phase transitions are governed by the first and second laws of thermodynamics under the constraints of mass and heat transport. The chemical potential of all components in all possible phases is therefore needed to estimate phase distributions of the different components as a basis for evaluation of risk for hydrate, ice, and other short or long-term problems of water with dissolved acidic components, like for instance rust.

Received: March 20, 2015
Accepted: September 1, 2015

DOI: 10.1021/acs.jced.5b00267
J. Chem. Eng. Data XXXX, XXX, XXX−XXX

Publication Date (Web): September 9, 2015 | doi: 10.1021/acs.jced.5b00267

Minimizing free energies in order to find the directions of progress and the dynamic distributions of components over the possible phases also imposes other constraints on the reference level for thermodynamic properties, which should be uniform for all components in all phases. This implies that ideal gas is the only feasible reference choice for all components distributed over the CO_2, water, hydrate, and adsorbed phases on mineral surfaces.

The main purpose of this work was to put together the general ideas forming our approach to evaluation of chemical potential by combining the Gibbs−Duhem relation with Gibbs free energy formulation (section 2). The proposed technique is then verified by applying it to a well-studied system involving water and methane. In section 3, we extend this treatment to a system highly relevant for carbon dioxide transport (water and H_2S dissolved in CO_2). These calculations are more complex due to the low solubility of these components. The conclusions are in section 4.

2. MOLECULAR DYNAMICS FOR THE CALCULATION OF CHEMICAL POTENTIAL AND FREE ENERGY

A molecular dynamics (MD) simulation in its basic formulation is a straightforward numerical integration of the motion of individual molecules governed by Newton's second law of classical mechanics where the force on the individual atom comes from its interactions with atoms of surrounding molecules. This integration corresponds to an isolated system with constant number of molecules, volume of the system, and total internal energy (NVE or microcanonical ensemble). In the case of a canonical ensemble, i.e., a system kept at constant temperature through a thermal contact with much larger heat bath but still mechanically isolated and not allowed to exchange mass with the surroundings (NVT system), it is nontrivial but possible to derive the governing equations from rigorous statistical mechanic considerations.[2−4] The use of the Nose−Hoover method and the canonical ensemble instead of simple temperature rescaling approach is desirable for at least two reasons, preserving the coupling between macro-physics and statistical mechanics, and obeying the constraints that statistical mechanics imposes on the way we control the simulations. Since statistical mechanics is the bridge from the nanoscale simulations to macro-scale thermodynamics, it is of crucial importance to ensure that we truly sample from the canonical ensemble and thus can make use of thermodynamic relationships that relate molecular dynamics samplings to macroscopic thermodynamic properties. This means that the probability distributions in both the momentum and the configurational space have to reproduce the canonical distributions in NVT simulations.

A number of direct and indirect conclusions and results can be derived from a MD investigation. The position and velocities of molecules can supply qualitative information on the specific way they interact and form structures. Particle motions and interactions produce statistical data on the microscopic scale that can be used to determine macroscale thermodynamic quantities such as pressure and temperature through the application of statistical mechanics concepts. To draw reliable macroscopic conclusions from microscopic MD data, it is very important that the sampled data should correspond to the appropriate statistical ensemble.

The configurational space (or volume space) is generally very complex since the fields from multiple atoms affect the interactions between the different atoms. For instance, in the simple case of monatomic atoms, the interactions between each pair will be affected by the presence of the field of the third one, and so on. These many-body correlations can be treated explicitly by ab initio techniques but are difficult to incorporate in classical molecular dynamics, so in practice the approximation of pairwise additive potential interaction is a compromise between complexity and the possibility to simulate large enough ensembles.

Each molecule is represented by a molecular model that contains data on the types of atoms, the intramolecular bonds, electrical charge distribution, mass, and geometric structure. MD simulations account for different intermolecular forces, and their effects on movement are determined by Newton's second law of motion. The first force is the Coulomb interaction distribution based on the charge distributions. The Coulomb potential U_{ij}^{coul} is given by

$$U_{ij}^{\mathrm{coul}} = \frac{q_i q_j}{4\pi\varepsilon_0 r_{ij}} \tag{1}$$

where the indices i and j represent two sites a distance r_{ij} apart with electrical charges q_i and q_j and ε_0 is the electric permittivity of free space.

Pauli repulsion and van der Waals attraction were approximated through the Lennard−Jones potential[5] given by the equation below,

$$U(r_{ij}) = 4\varepsilon\left[\left(\frac{\sigma}{r_{ij}}\right)^{12} - \left(\frac{\sigma}{r_{ij}}\right)^{6}\right] \tag{2}$$

which has a characteristic well shape. At interaction distance $r_{ij} < \sigma$, the repulsive term will ensure nonoverlap of atoms, with the van der Waals attraction dominating elsewhere. The well depth ε and well Lennard−Jones diameter σ constitute the force field parameters for molecular model employed.

In this article, we have used four different molecular force fields. The models involved the TIP4P model for water,[6] H_2S model due to Kristóf and Liszi,[7] the EPM2 model for CO_2,[8] and single-site model by Jorgensen et al.[9] for methane. The cross-term interactions between unlike sites were calculated through a straightforward application of Lorentz−Berthelot rules, without any additional correction factors involved.

While the potential interaction energy is easily by direct sampling of properties generated during a simulation run, an evaluation of chemical potential will generally necessitate a thermodynamic integration scheme of some sorts.[4] Finding an approach equally applicable for estimation of chemical potential for mixtures involving very different species (water, hydrogen sulfide, CO_2) dissolved into each other at varying concentrations (including infinite dilution) poses a set of unique challenges due to poor solute statistics.

2.1. Temperature Integration Method. One option is to use the direct temperature integration method. Molecular dynamic simulations of the system of interest are performed at base temperature T_0 as well as a series of temperature points between T_0 and a sufficiently high temperature. This procedure is applied to obtain the total potential energy of the system, $U_{\mathrm{tot}}(T^{-1})$, as a function of inverse temperature, with $U_{\mathrm{tot}}(0) = 0$. An example of such a curve is shown in Figure 1. To obtain the chemical potential, U_{tot} is numerically integrated from 0 to T_0^{-1} and multiplied by T_0.

2.2. Polynomial Path Method. Thermodynamic integration over a polynomial path is an alternative formulation of the general thermodynamic integration approach introduced by Mezei.[10] Here the studied system is tethered to an equivalent ideal gas system through a parameter λ, where $\lambda = 0$ corresponds

DOI: 10.1021/acs.jced.5b00267
J. Chem. Eng. Data XXXX, XXX, XXX−XXX

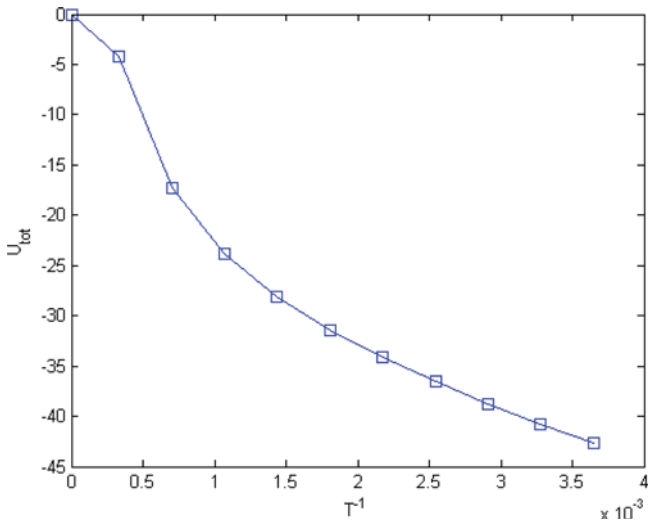

Figure 1. An example of temperature integration at T_0 = 274.15 K for two H_2S molecules dissolved in 512 water molecules.

to the ideal gas system, while $\lambda = 1$ yields to the studied system. Molecular dynamic simulations are conducted on hybrid systems with λ between 0 and 1. λ is a scaling parameter for the interaction energy U, which comprised of a short-range interaction term and additional long-range Coulumbic contributions for all species except methane. The specific force fields employed in this study are listed later in this section. The energy term U for the hybrid system is given by

$$U(\lambda) = \lambda^{k_1}U_1 + \lambda^{k_6}U_6 + \lambda^{k_{12}}U_{12} \tag{3}$$

where U_1, U_6, and U_{12} represent energy terms with the corresponding dependence on the inverse distance between molecular sites, r^{-1} (Coulomb), r^{-6} (van der Waals), and r^{-12} (Pauli), respectively. Parameters k_1, k_6, and k_{12} can theoretically be chosen arbitrarily, with the final result being in principle independent of the selection. In practice, these parameters will govern the rate at which each individual contribution is dampened, and the accuracy of the integration can be affected by an insufficient sampling of the available phase space. After a preliminary investigation focusing on a pure water system, we have chosen the combination $k_1 = 3$, $k_6 = 2$, and $k_{12} = 4$, which were used for all the subsequent simulation sets.

MD simulations have been run for the selected set of λ-values that are, in the case of a three point integration, $\lambda = 0.1125$, 0.5, and 0.8875 with the estimate for $\langle \partial U/\partial\lambda \rangle$ calculated by the simulation program for each point. The residual Helmholtz free energy A is then obtained by numeric integration.

$$A = \int_0^1 \left\langle \frac{\partial U}{\partial \lambda} \right\rangle \mathrm{d}\lambda \tag{4}$$

The integration is done by fitting a polynomial over the selected nodes. Error estimates in the integration were obtained by conducting the integration several times with a random normal-distributed perturbation of $\langle \partial U/\partial\lambda \rangle$ at each node in order to obtain an estimate for the uncertainty in A. The issue of determining the value and uncertainty of integrals from data points with uncertainty was discussed extensively in Cordero et al.[11]

While we found that the application of either temperature integration, simple linear scaling of potential or integration along a polynomial path yields reliable results for bulk fluids, attempts to evaluate chemical potential of few solute molecules dissolved in the solvent bulk have proven to yield highly inaccurate estimates with uncertainties often exceeding the absolute value of integrands. The two integration methods are mentioned here for completeness since the result for pure water and pure carbon dioxide were obtained using eq 4 and Mezei algorithm,[10] while eq 3 has been applied for water adsorbed onto hematite.[17]

Trying to reduce the statistical noise by drastically increasing the number of solute molecules would necessitate using extremely large systems but not necessarily guarantee success. We have therefore considered an alternative approach that allows one to analyze a much better behaving property of the system based on the Gibbs−Duhem equation. Out of the three methods tested in this work, it was the Gibbs−Duhem method that proved to be the most satisfactory for our particular situation.

2.3. Chemical Potential Estimation via Gibbs−Duhem Relation. The famous Gibbs−Duhem relation is simply a consistency criterion that arises from the full differentiation of Gibbs free energy in terms of all the thermodynamic variables. Comparing this result with the combined first and second laws of thermodynamics results in a sum of terms in the pure mathematical derivation that has to be zero. In the context of this work, we do not have to consider all variables, since we either fix volume and temperature in the NVT ensemble simulations or fix pressure and temperature in the NPT ensemble. From either ensemble, the result is the same, but the independent variables vary with ensemble

$$\mu_1 = \left(\frac{\partial \underline{U}}{\partial N_i}\right)_{S,\underline{V}} = \left(\frac{\partial \underline{A}}{\partial N_i}\right)_{T,\underline{V}} = \left(\frac{\partial \underline{G}}{\partial N_i}\right)_{T,P} \tag{5}$$

Where the first version on right-hand side corresponds to the microcanonical ensemble, the second term corresponds to the canonical ensemble, and the third one corresponds to the NPT ensemble. Lines under symbols means extensive quantities (dependent on the size of the sample), and N is number of molecules with type index i.

In this work we only conduct simulations in the NVT or NPT ensemble, so only the two latest relationships are of interest here. For the canonical ensemble that the NVT simulations aim to reproduce, the combined first and second laws of thermodynamics yield the following:

$$\mathrm{d}\underline{A}^{(s)}(T, V, \vec{N}) \leq -\underline{S}^{(s)}\mathrm{d}T^{(e)} - P^{(s)}\mathrm{d}\underline{V}^{(s)} + \sum_{i=1}^{n} \mu_i^{(s)}\mathrm{d}N_i^{(s)} \tag{6}$$

where superscript "(s)" denotes the system in consideration and superscript "(e)" denotes the surroundings. N is the number of different molecules in the ensemble. The arrow above N indicates the vector containing mole numbers of all components in the ensemble. The equality in eq 6 is valid at equilibrium.

In the NVT ensemble, the volume is fixed, while the temperature is controlled and regarded as constant, although it fluctuates within temperature control boundaries in a molecular simulation. For any given temperature and volume it follows directly from eq 5, since the molar dependencies in Helmholtz free energy are linear, that

$$\underline{A}^{(s)}(T, V, \vec{N}) = \sum_{i=1}^{n} \mu_i^{(s)}(T, V, N)N_i^{(s)} \tag{7}$$

Publication Date (Web): September 9, 2015 | doi: 10.1021/acs.jced.5b00267

DOI: 10.1021/acs.jced.5b00267
J. Chem. Eng. Data XXXX, XXX, XXX−XXX

Table 1. Helmholtz Free Energies for Methane Dissolved in Water

TIP4P molecules	CH_4 molecules	Helmholtz free energy (A) (kJ·mol^{-1})	μ_{H2O} (kJ·mol^{-1})	μ_{CH4} (kJ·mol^{-1})
512	0	−24.17 ± 0.02	−26.48	10.14
504	8	−23.61 ± 0.02	−26.49	10.12
496	16	−23.06 ± 0.02	−26.52	10.10
488	24	−22.46 ± 0.02	−26.49	10.13

Direct differentiation of eq 7 gives

$$\mathrm{d}\underline{A}^{(s)}(T, V, \vec{N}) = \sum_{i=1}^{n} \mu_i^{(s)}(T, V, N)\mathrm{d}N_i^{(s)} + \sum_{i=1}^{n} N_i^{(s)}\mathrm{d}\mu_i^{(s)}(T, V, N) \quad (8)$$

Combining eqs 6 and 8 gives directly the Helmholtz free energy version of Gibbs−Duhem:

$$\sum_{i=1}^{n} N_i^{(s)}\mathrm{d}\mu_i^{(s)}(T, V, N) = -\underline{S}^{(s)}\mathrm{d}T^{(e)} - P^{(s)}\mathrm{d}\underline{V}^{(s)} \quad (9)$$

Dividing by total mole numbers for constant T and V, we arrive at the two-component version, for mixtures of water and carbon dioxide:

$$x_{H_2O}\mathrm{d}\mu_{H_2O}(T, V, \vec{N}) + x_{CO_2}\mathrm{d}\mu_{CO_2}(T, V, \vec{N}) = 0 \quad (10)$$

Similar derivation in the NPT ensemble leads to

$$x_{H_2O}\mathrm{d}\mu_{H_2O}(T, P, \vec{N}) + x_{CO_2}\mathrm{d}\mu_{CO_2}(T, P, \vec{N}) = 0 \quad (11)$$

Equations 6 and 7 also apply to residual properties (the real property minus the ideal gas value at same conditions). Using superscript "res" to denote residual property and applied to eq 10:

$$x_{H_2O}\mathrm{d}\mu_{H_2O}^{res}(T, V, \vec{N}) + x_{CO_2}\mathrm{d}\mu_{CO_2}^{res}(T, V, \vec{N}) = 0 \quad (12)$$

$$x_{H_2O}\mu_{H_2O}^{res}(T, V, \vec{N}) + x_{CO_2}\mu_{CO_2}^{res}(T, V, \vec{N}) = A^{res} \quad (13)$$

For the two-component system of H_2O and CO_2, the conservation of mole-fractions implies:

$$\mathrm{d}x_{H_2O} + \mathrm{d}x_{CO_2} = 0 \quad (14)$$

Combinations of eqs 12, 13, and 14 lead to

$$\mu_{H_2O}^{res}(T, V, \vec{N}) - \mu_{CO_2}^{res}(T, V, \vec{N}) = \frac{\mathrm{d}A^{res}}{\mathrm{d}x_{H_2O}} \quad (15)$$

Conducting NVT simulations for different concentrations and integrating sampled interaction energies using either temperature integration or an algorithm for scaling the interaction energies provides a route to chemical potentials for both components.

From the relationship between Gibbs free energy and Helmholtz free energy, it directly follows that

$$G^{res}(T, P, \vec{N}) = A^{res}(T, V, \vec{N}) + (PV)^{res} \quad (16)$$

The difference between G and A is the difference between enthalpy H and energy U. These are both state functions, so the difference between G and A are as well. This also holds for residual properties. This implies that the latter contribution can be evaluated separately and added, as was done by Kvamme et al.[1] But it is also possible to integrate sampled interaction energies separately as in NVT and add sampled values for PV. In this case the pressure should be kept as control pressure and the sampled system volumes must be averaged and applied in the corresponding residual term:

$$(PV)^{res} = (PV - RT) \quad (17)$$

The corresponding ideal gas chemical potentials can easily be evaluate from the momentum-space canonical partition function. In the case of flexible molecules, the required translational contribution and components of inertia tensor will be given by their averaged values, sampled throughout the simulation. For rigid models such as TIP4P, the moments of inertia will remain fixed.

Verification of the Approach: Chemical Potential of Methane at Infinite Dilution in Water. The molecular dynamics simulations were conducted using the MDynaMix[12] program package. The results of these simulations were used to calculate chemical potentials and free energy.

Molecular dynamics simulations for methane dissolved in water were conducted to verify the approach outlined. Methane solubility in water is larger than water in methane, allowing one to use higher concentrations to make it easier to obtain more accurate data for the same system size.

Thermodynamic integration using the Mezei polynomial path approach and Gibbs−Duhem was used to find the Helmholtz free energy of a 512 molecule system with four different concentrations of methane, 0, 8, 16, and 24 molecules.

The results in Table 1 are displayed graphically in Figure 2. Since the curve appears to be almost linear, we fitted the

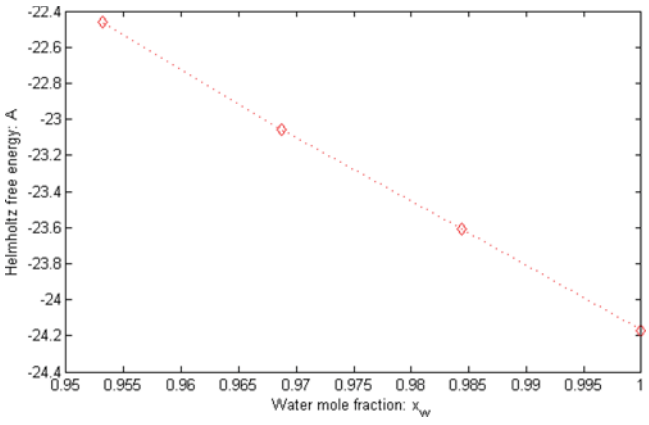

Figure 2. Helmholtz free energy, A, of the water−methane system as a function of water molar fraction, x_w.

Helmholtz free energy at this concentration range to the following linear equation:

$$A^{(1)}(x_{H_2O}) \approx -36.62x_{H_2O} + 12.42 \quad (18)$$

We have two equations for the two unknown chemical potentials μ_{H_2O} and μ_{CH_4} for each mole mole fraction. Combining eqs 5 and 7 (the Gibbs−Duhem relation) yields the equation set

$$x_{H_2O}\mu_{H_2O} + x_{CH_4}\mu_{CH_4} = A^{(1)}(x_{H_2O}) - RT \quad (19)$$

DOI: 10.1021/acs.jced.5b00267
J. Chem. Eng. Data XXXX, XXX, XXX−XXX

$$\mu_{H_2O} - \mu_{CH_4} = \frac{dA^{(1)}}{dx_{H_2O}} \quad (20)$$

Equation 20 is independent of the concentration since $A^{(1)}(x_{H_2O})$ could be approximated by a linear function. Had that not been the case, we would have needed to calculate $(dA^{(1)}/dx_{H_2O})$ for each value of x_{H_2O}.

From these equations we calculated the chemical potentials for the water and methane species presented in Table 1. The results agree very well with the theoretic expectations as well as the estimates from[13] that found $\mu_{CH_4} = 10.5 \pm 1.7$ kJ·mol^{-1}.

Water and H_2S in CO_2. Water has a low solubility in any gas since hydrogen bonding gives water molecules a strong tendency to cluster together. The solubility is somewhat higher in CO_2 than it is in air, but it is still much lower than the solubility of CO_2 in water. The mutual solubilities of these fluids have been subject to extensive study. Spycher et al.[14] has an appendix with a table of solubilities for various pressure and temperature conditions. Generally, the solubility of water in CO_2 at typical pipeline temperatures, usually (2 to 5) °C, is in the order of 2000 ppmv.

In a molecular dynamics simulation, a presence of water above the solubility limit results in an eventual (but not immediate) clustering of the water droplets. This consideration required us to employ systems with at least 500 molecules to accommodate multiple water molecules.

The structure of H_2S molecules resembles that of water molecules, the important differences including much weaker polarity and inability to form hydrogen bonds. Our method to handle H_2O and H_2S dissolved in dense CO_2 is described in the next sections.

3. INFINITE DILUTION AND PURE CARBON DIOXIDE PROPERTIES

3.1. Molar Volume of H_2S. The geometry and partial charge distribution of H_2S molecules are very different from that of the CO_2, and the presence of H_2S molecules can therefore lead to significant restructuring of packing in the CO_2 fluid. Consequently, adding H_2S molecules can affect the total volume in a far from straightforward manner; in some cases structural changes caused by the presence of H_2S molecules may cause the total volume to actually decrease. This renders useless any attempt at using the direct method for finding the partial molar volume. A more general method for estimating the volume is via the radial distribution functions (RDF), and we applied an approach to calculate the molar volume of H_2S in CO_2. Figure 3 shows the RDF between H_2S and CO_2 calculated from a simulation involving 4 H_2S molecules and 996 CO_2 molecules. To determine the molar volume, we have used the first shell approach, as given by

$$v_m = 4\pi \int_0^{r(g_{max})} g(r) r^2 dr \quad (21)$$

where $r(g_{max})$ is the location for the first peak of $g(r)$. In case of H_2S the sulfur atom in H_2S versus oxygen in CO_2 dominates the volume occupied by the H_2S molecule. The partial molar volume was calculated from a simulation with 4 H_2S molecules and 996 CO_2 molecules. The radial distribution function for sulfur versus oxygen is plotted in Figure 3. In this case, the first peak can be found at about 3.55 Å, and an evaluation of the integral gave a molar volume of 31.4 Å^3/molecule or about 18.9 cm^3 per mole. This corresponds to a density of 1.8 kg/dm^3.

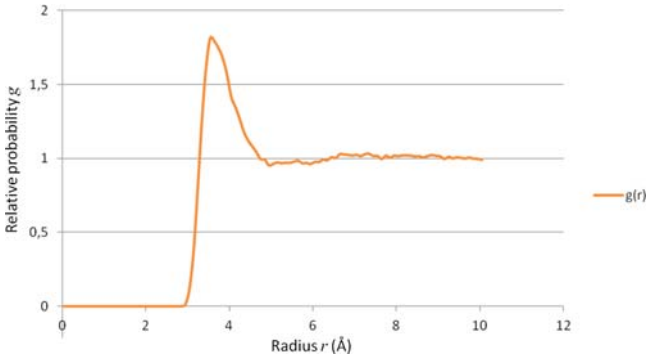

Figure 3. Radial distribution function for H_2S sulfur and CO_2 oxygen in case of hydrogen sulfide dissolved in carbon dioxide. A temperature of 274.15 K and density of 0.94802 g·cm^{-3} corresponded to pressure of 70 atm.

3.2. Chemical Potentials and Free Energy at Finite Dilution. The mixture free energy change for H_2S, from the reference states for CO_2 (pure CO_2 liquid state) and infinite dilution of H_2S (similar for H_2O) in CO_2 can be written as

$$G^M(T, P, \vec{x}_{CO_2}) = G(T, P, \vec{x}_{CO_2}) - x_{CO_2}\mu^{pure}_{CO_2,CO_2}(T, P) - (1 - x_{CO_2,CO_2})\mu^{\infty}_{H_2S,CO_2}(T, P) - RT \ln x_{CO_2,CO_2} - RT \ln[1 - x_{CO_2,CO_2}] = RT \ln[\gamma^{\infty}_{H_2S,CO_2}(T, P, \vec{x}_{CO_2})] \quad (22)$$

Tables 2 and 3 contain the values of chemical potential for fluid CO_2 with dissolved water (Table 2) and H_2S (Table 3), derived from molecular dynamics simulations.

The Van Laar equation[15] has proven to be accurate enough for water dissolved into CO_2. Given reference chemical potentials for CO_2, H_2S, and water, one may therefore apply it within the validity limits of eq 22 to fit the estimates in Table 2 and Table 3 into a sufficiently flexible model for the activity coefficients of H_2S and H_2O, respectively.

$$\ln[\gamma^{\infty}_{i,CO_2}(T, P, \vec{x}_{CO_2})] = \frac{G^M(T, P, \vec{x}_{CO_2})}{RT} = \frac{\alpha(T)}{\left(1 + \left[\frac{\alpha(T)x_{i,CO_2}}{\beta(T)(1 - x_{i,CO_2})}\right]\right)^2} \quad (23)$$

where i is either H_2O or H_2S, and corresponding temperature and pressure dependencies of α and β are fitted by the following expression with parameters p_i listed in Table 4 below for each mixture. Subscript "*critical*" denotes a critical point, with additional subscript indicating CO_2, i.e., $T_{critical,CO_2} = 304.19$ K and $P_{critical,CO_2} = 73.80$ bar.

$$\chi_j = p_0 + p_1x^{0.25} + p_2x^{0.5} + p_3x^{0.75} + p_4x + p_5x^{1.5} + p_6x^2 + p_7x^3 + p_8y^{0.5} + p_9y + p_{10}y^2 + p_{11}y^3 + p_{12}w$$
$$\chi_1 = \alpha, \quad \chi_2 = \beta \quad (24)$$

$$x = \frac{T_{critical,CO_2}}{T} \quad (25)$$

$$y = \left(\frac{P}{P_{critical,CO_2}} - 1\right) \quad (26)$$

Publication Date (Web): September 9, 2015 | doi: 10.1021/acs.jced.5b00267

DOI: 10.1021/acs.jced.5b00267
J. Chem. Eng. Data XXXX, XXX, XXX−XXX

Table 2. Molar Gibbs Free Energy Estimates for Different Concentrations of H_2S Dissolved into CO_2 at Temperatures between (274.15 and 283.15) K and Pressures between (100 and 200) bar[a]

T/K	P/bar	x_{H_2S}	ideal contribution to chemical potential	residual chemical potential	ideal mixture free energy	total chemical potential
274.15	100	0	−41.1705	−4.0411	0	−45.2116
274.15	100	0.0010	−41.1604	−4.0442	−0.0180	−45.2226
274.15	100	0.0020	−41.1503	−4.0405	−0.0329	−45.2237
274.15	100	0.0030	−41.1402	−4.0527	−0.0466	−45.2395
274.15	100	0.0500	−40.6662	−4.1897	−0.4525	−45.3084
278.15	100	0	−41.9379	−3.9160	0	−45.8539
278.15	100	0.0010	−41.9276	−3.9196	−0.0183	−45.8655
278.15	100	0.0020	−41.9173	−3.9208	−0.0334	−45.8715
278.15	100	0.0030	−41.9070	−3.9270	−0.0472	−45.8812
278.15	100	0.0040	−41.8967	−3.9229	−0.0603	−45.8799
278.15	100	0.0500	−41.4229	−4.0630	−0.4591	−45.9450
283.15	100	0	−42.9101	−3.7534	0	−46.6638
283.15	100	0.0010	−42.8995	−3.7745	−0.0186	−46.6926
283.15	100	0.0020	−42.8889	−3.7610	−0.0340	−46.6839
283.15	100	0.0030	−42.8784	−3.7685	−0.0481	−46.6950
283.15	100	0.0500	−42.3811	−3.9050	−0.4674	−46.7535
274.15	150	0	−41.1110	−4.0772	0	−45.1882
274.15	150	0.0010	−41.1010	−4.0780	−0.0180	−45.1970
274.15	150	0.0020	−41.0909	−4.0822	−0.0329	−45.2060
274.15	150	0.0030	−41.0809	−4.0866	−0.0466	−45.2141
274.15	150	0.0500	−40.6096	−4.2211	−0.4525	−45.2832
278.15	150	0	−41.8707	−3.9618	0	−45.8325
278.15	150	0.0010	−41.8605	−3.9593	−0.0183	−45.8381
278.15	150	0.0020	−41.8502	−3.9555	−0.0334	−45.8391
278.15	150	0.0030	−41.8400	−3.9659	−0.0472	−45.8531
278.15	150	0.0500	−41.3591	−4.1048	−0.4591	−45.9230
283.15	150	0	−42.8253	−3.8175	0	−46.6428
283.15	150	0.0010	−42.8141	−3.8120	−0.0186	−46.6447
283.15	150	0.0020	−42.8029	−3.8168	−0.0340	−46.6537
283.15	150	0.0030	−42.7938	−3.8207	−0.0481	−46.6626
283.15	150	0.0500	−42.3006	−3.9556	−0.4674	−46.7236
274.15	200	0	−41.0615	−4.1035	0	−45.1650
274.15	200	0.0010	−41.0515	−4.1087	−0.0180	−45.1782
274.15	200	0.0020	−41.0415	−4.1102	−0.0329	−45.1846
274.15	200	0.0030	−41.0316	−4.1093	−0.0466	−45.1875
274.15	200	0.0500	−40.5626	−4.2565	−0.4525	−45.2716
278.15	200	0	−41.8151	−3.9951	0	−45.8102
278.15	200	0.0010	−41.8049	−3.9795	−0.0183	−45.8027
278.15	200	0.0020	−41.7947	−4.0260	−0.0340	−45.8541
278.15	200	0.0030	−41.7846	−3.9997	−0.0472	−45.8315
278.15	200	0.0500	−41.3062	−4.1334	−0.4591	−45.8987
283.15	200	0	−42.7620	−3.8495	0	−46.6115
283.15	200	0.0010	−42.7509	−3.8569	−0.0186	−46.6264
283.15	200	0.0020	−42.7398	−3.8484	−0.0340	−46.6222
283.15	200	0.0030	−42.7307	−3.8591	−0.0481	−46.6379
283.15	200	0.0500	−42.2404	−3.9880	−0.4674	−46.6958

[a]Molar free energies and chemical potentials in units of kJ·mol^{-1}.

$$w = \ln\left(\frac{P}{P_{\text{critical},CO_2}}\right) \tag{27}$$

3.3. Chemical Potential at Infinite Dilution. The infinite-dilution chemical potentials for H_2S and H_2O dissolved in CO_2 can be estimated from the Gibbs−Duhem relation. In the case of H_2S in CO_2 mixture, the following equations can be used

$$G(T, P, \vec{x}) = x_{H_2S,CO_2}\mu_{H_2S,CO_2}(T, P, \vec{x}) + (1 - x_{H_2S,CO_2})\mu_{CO_2,CO_2}(T, P, \vec{x}) \tag{28}$$

$$\frac{dG(T, P, \vec{x})}{dx_{H_2S,CO_2}} = \mu_{H_2S,CO_2}(T, P, \vec{x}) - \mu_{CO_2,CO_2}(T, P, \vec{x}) \tag{29}$$

$$\mu^{\infty}_{H_2S,CO_2}(T, P, \vec{x}) = G(T, P, x_{H_2S,CO_2} \to 0) + \lim\left[\frac{dG(T, P, \vec{x})}{dx_{H_2S,CO_2}}\right]_{x_{H_2S,CO_2}\to 0} \tag{30}$$

Table 5 below lists chemical potential values of H_2S and water at infinite dilution in CO_2, and H_2S and CO_2 at infinite dilution in water for temperatures of (274.15, 278.15, and 283.15) K

DOI: 10.1021/acs.jced.5b00267
J. Chem. Eng. Data XXXX, XXX, XXX−XXX

Table 3. Molar Gibbs Free Energy Estimates for Different Concentrations of H_2O Dissolved into CO_2 at Temperatures between (274.15 and 283.15) K and Pressures between (100 and 200) bar[a]

T/K	P/bar	x_{H_2O}	ideal contribution to chemical potential	residual chemical potential	ideal mixture free energy	total chemical potential
274.15	100	0	−41.1705	−4.0411	0	−45.2116
274.15	100	0.0010	−41.1572	−4.0474	−0.0180	−45.2226
274.15	100	0.0020	−41.1440	−4.0490	−0.0329	−45.2259
278.15	100	0	−41.9379	−3.9160	0	−45.8539
278.15	100	0.0010	−41.9239	−3.9212	−0.0183	−45.8634
278.15	100	0.0020	−41.9098	−3.9288	−0.0334	−45.8720
283.15	100	0	−42.9101	−3.7534	0	−46.6638
283.15	100	0.0010	−42.8957	−3.7602	−0.0186	−46.6745
283.15	100	0.0020	−42.8813	−3.7728	−0.0340	−46.6881
274.15	150	0	−41.1110	−4.0772	0	−45.1882
274.15	150	0.0010	−41.0972	−4.0775	−0.0180	−45.1927
274.15	150	0.0020	−41.0836	−4.0739	−0.0329	−45.1904
278.15	150	0	−41.8707	−3.9618	0	−45.8325
278.15	150	0.0010	−41.8567	−3.9612	−0.0183	−45.8362
278.15	150	0.0020	−41.8428	−3.9556	−0.0334	−45.8318
283.15	150	0	−42.8253	−3.8175	0	−46.6428
283.15	150	0.0010	−42.8110	−3.8120	−0.0186	−46.6416
283.15	150	0.0020	−42.7967	−3.8264	−0.0340	−46.6571
274.15	200	0	−41.0615	−4.1035	0	−45.1650
274.15	200	0.0010	−41.0478	−4.0985	−0.0180	−45.1643
274.15	200	0.0020	−41.0342	−4.0985	−0.0329	−45.1656
278.15	200	0	−41.8151	−3.9951	0	−45.8102
278.15	200	0.0010	−41.8012	−3.9853	−0.0183	−45.8048
278.15	200	0.0020	−41.7873	−3.9884	−0.0334	−45.8091
283.15	200	0	−42.7620	−3.8495	0	−46.6115
283.15	200	0.0010	−42.7478	−3.8434	−0.0186	−46.6098
283.15	200	0.0020	−42.7335	−3.8493	−0.0340	−46.6168

[a]Molar free energies and chemical potentials in units of kJ·mol^{-1}.

Table 4. Estimated Parameters for the Activity Coefficient Model

	liquid CO_2 as solvent				liquid H_2O as solvent			
	H_2S in CO_2		H_2O in CO_2		H_2S in H_2O		CO_2 in H_2O	
P_{ar}	α	β	A	β	α	β	α	B
P_0	−6.29679	0.288660	1.364860	2.162614	10.39154	5.93381	19.8669	1.12020
P_1	−15.20220	0.382388	1.617741	2.284311	8.16632	5.09487	16.3994	0.817279
P_2	−14.85513	0.258199	1.718498	2.412527	3.07683	5.32093	9.37871	1.60096
P_3	−6.59852	0.337460	1.719525	2.547452	0.823095	4.00474	5.33695	0.863331
P_4	−3.45982	0. 391720	1.615094	2.689282	1.24715	3.79870	4.13601	1.25930
P_5	12.56425	0.1619333	0.993433	2.994444	−31.10236	−1.63870	−32.8595	−2.93810
P_6	30.39946	0.3651374	−0.233033	3.480842	15.11738	0.719982	11.2212	0.82178
P_7	70.11823	−0.6098141	−4.482085	4.647000	−2.35571	−2.01386	−24.6482	1.21390
P_8	−10.08153	−0.7580262	2.115442	−9.594403	5.26819	2.96550	3.83776	0.465034
P_9	−1.00630	−0.0345400	2.160482	−10.117969	−4.40282	−4.46144	−11.2329	−5.29186
P_{10}	21.31552	0.07581578	0.389556	−7.819354	4.13675	−1.50466	0.909059	0.667554
P_{11}	41.52672	0.116916	−1.969798	−9.004456	−2.73952	−5.07581	2.90284	0.809065
P_{12}	−7.02318	−0.147903	0.395813	−10.098084	−4.01203	−2.07967	−8.18088	−3.23253
P_{13}	−62.02840	0.0675898	1.869470	−8.706712	3.73011	5.15416	6.12426	0.224087

and pressures of (100, 150, and 200) bar based on data of Tables 2 and 3.

The pressure dependency of γ_{i,CO_2} is expected to be similar to that of water.[16] Coefficients for eq 28−30 are given in Table 4. The pure CO_2 chemical potential can be fitted to eq 31 below, with the parameters listed in Table 6.

$$\mu_{CO_2}^{pure} = k_0(1 + a_6 z^{0.5} + a_7 z + a_8 z^{1.5} + a_9 z^2 + a_{10} z^3 + b_4 q^{0.5} + b_5 q + b_6 q^{1.5} + b_7 q^2 + b_8 q^3)^{-1} \quad (31)$$

where:

$$z = \left(\frac{T}{T_{critical,CO_2}} + 0.08\right)^2 \quad (32)$$

$$q = \left(\frac{P}{P_{critical,CO_2}} + 0.3\right)^{-2.5} \quad (33)$$

DOI: 10.1021/acs.jced.5b00267
J. Chem. Eng. Data XXXX, XXX, XXX−XXX

Table 5. Estimated Infinite Dilution Chemical Potentials for H_2S Dissolved in Carbon Dioxide and Water

		liquid CO_2 as solvent		liquid H_2O as solvent	
T/K	P/bar	$\mu^{\infty}_{H_2S,CO_2}$ (kJ·mol^{-1})	$\mu^{\infty}_{H_2O,CO_2}$ (kJ·mol^{-1})	$\mu^{\infty}_{H_2S,CO_2}$ (kJ·mol^{-1})	$\mu^{\infty}_{CO_2S,HO_2}$ (kJ·mol^{-1})
274.15	100	−61.16	−55.71	−56.90	−58.02
278.15	100	−58.83	−55.80	−56.39	−57.86
283.15	100	−56.00	−55.91	−55.80	−57.68
274.15	150	−53.89	−53.09	−56.78	−56.41
278.15	150	−53.73	−53.58	−56.28	−56.17
283.15	150	−53.54	−54.18	−55.68	−55.89
274.15	200	−46.61	−43.46	−58.11	−54.80
278.15	200	−46.46	−43.96	−57.54	−54.48
283.15	200	−46.27	−44.56	−56.85	−54.09

Table 6. Estimated Parameters for eq 31 for Pure CO_2 for Temperature 274.15 K and Pressures Ranging from (100 to 200) bar

pure liquid CO_2 solvent chemical potential (kJ·mol^{-1})	
k_0	−42.548
a_6	0.14186
a_7	0.049729
a_8	0.065648
a_9	−0.36044
a_{10}	−0.00056083
b_4	0.21436
b_5	−0.45825
b_6	0.00016359
b_7	0.47533
b_8	0.15225

Similar values for pure liquid water have taken from Kvamme and Tanaka.[18] Note that those values are for 1 bar but are trivially corrected to the appropriate pressure using a constant density of 1000 kg/m^2.

An important advantage of infinite dilution properties based on molecular simulations is that these values have ideal gas as reference. In conjunction with our earlier estimated values for water chemical potential in empty hydrate structures from Kvamme and Tanaka,[18] data presented in this work opens up for free energy description of all components in all phases, which is very convenient for use in phase field theory[16] analysis of competing phase transitions in nonequilibrium systems.

Another aspect that needs to be investigated is related to the low partial density of water dissolved in CO_2, which typically ranges from 400 kg·m^{-3} to 650 kg·m^{-3} for the conditions of pressures, temperatures, and compositions investigated in this study. The question is whether water prefers to dissolve in CO_2 as dimers or higher number of water in clusters rather than being dissolved into CO_2 as uniformly distributed water monomers. This can also be investigated through free energy evaluations using particle interaction scaling. One way is to introduce one or more ideal gas water molecules close to the monomer and scale up the interaction for calculation of chemical potentials. A scheme for converting CO_2 molecules into water molecules and calculating related free energy changes is also feasible.

4. CONCLUSIONS

By combining the Gibbs−Duhem equation and the Gibbs free energy, we have presented a method for calculating individual chemical potentials of each component in a solution by considering chemical potential values estimated for systems at varying concentrations. The validity of the method has been verified for a solution of methane in water by way of comparison to estimates done by other groups and experimental data from literature.

This method was then applied to investigate H_2S and H_2O dissolved in carbon dioxide. While the higher polarity and lower solubility make these solutions more difficult to study, we have nonetheless found parameters for the chemical potential at infinite dilution for these systems under the conventional assumption of uniform solution. These infinite dilution chemical potentials provide a consistent basis for fitting experimental solubility data within absolute thermodynamics (ideal gas as reference state). This approach provides a very convenient tool for schemes that involve analysis of Gibbs free energy for nonequilibriums systems. Phase field theory (PFT), a powerful technique that requires minimization of free energy under constraints of mass and heat transport, is a natural candidate for this. Work is in progress on incorporating data presented here into a PFT model for analysis of hydrate risk during transport of CO_2 containing water and impurities.

We have also used data estimated by means of molecular modeling to evaluate different scenarios for water dropping out from dense CO_2. Specifically, the upper limit of water content that can be tolerated before water will form hydrate directly, and water adsorption onto hematite (rust), respectively, has been evaluated. Based on our earlier estimates for chemical potential of water in the vicinity of hematite,[17] adsorption will be the factor determining the limit of water acceptable in terms of hydrate risk.

The estimated partial molar density of water dissolved in CO_2 was found to be fairly low. This raises the question of whether water will thermodynamically benefit from dissolving into CO_2 as single water molecules or would prefer associating into water dimers or even larger clusters. Thermodynamically speaking, a single dissolved water molecule will differ from water in a water dimer or a trimer. If this is the case, then the existing procedures for estimating water solubility into liquid CO_2 must be revised accordingly, based on chemical potentials of water in CO_2 as monomers, dimers, trimers, and so on. Work is in progress to investigate this possibility.

AUTHOR INFORMATION

Corresponding Author

*E-mail: bjorn.kvamme@ift.uib.no.

Funding

We acknowledge the grant and support from Research Council of Norway through the following projects: SSC-Ramore, “Subsurface storage of CO_2 − Risk assessment, monitoring and remediation”, Research Council of Norway, project number: 178008/I30, FME-SUCCESS, Research Council of Norway, project number: 804831, and PETROMAKS, “CO2 injection for

extra production", Research Council of Norway, project number: 801445. Funding from Research Council of Norway, TOTAL and Gassco through the project "CO2/H2O+" is highly appreciated.

Notes

The authors declare no competing financial interest.

■ ACKNOWLEDGMENTS

Bjørnar Jensen and Kim Nes Leirvik at the University of Bergen have contributed to the framework and numerical modeling in the CO2/H2O+ project that has been used in this article.

■ NOMENCLATURE

a_{6-10}	Parameter in the equation for the pure chemical potential for CO_2
b_{4-8}	Parameter in the equation for the pure chemical potential for CO_2
A	Helmholtz free energy
e	The surroundings
ε_0	Electric permittivity of free space
ε	Lennard−Jones well depth
EP_{tot}	Total potential energy [kJ·mol^{-1}]
G	Gibbs free energy [kJ·mol^{-1}]
H	Enthalpy [kJ·mol^{-1}]
k	Parameter in the energy term for the hybrid system
k_0	Parameter in the equation for the pure chemical potential for CO_2
λ	Parameter in the energy term for the hybrid system
MD	Molecular dynamics
N	Number of molecules
p_i	Parameter in the activity coefficient model
P	Pressure [Pa]
q	Electric charge
r	Distance [m]
R	Molar gas constant [kJ·(K·mol)$^{-1}$]
σ	Lennard−Jones diameter
s	The system in consideration
S	entropy
T	Temperature [K]
U	Potential energy
V	Volume
w	ln(reduced pressure)
x	Inverse reduced temperature
x	Mole fraction
$\vec{x}$	Liquid composition
y	Reduced pressure −1
α	Liquid (water) phase fraction
β	Inverse of the gas constant times temperature
γ	Activity coefficient

■ REFERENCES

(1) Kvamme, B.; Kuznetsova, T.; Jensen, B.; Stensholt, S.; Bauman, J.; Sjoblom, S.; Nes Lervik, K. N. Consequences of CO2 solubility for hydrate formation from carbon dioxide containing water and other impurities. *Phys. Chem. Chem. Phys.* **2014**, *16*, 8623−8638.

(2) Nose, S. A unified formulation of the constant temperature molecular-dynamics methods. *J. Chem. Phys.* **1984**, *81*, 511−519.

(3) Hoover, W. G. Canonical dynamics: Equilibrium phase-space distributions. *Phys. Rev. A: At., Mol., Opt. Phys.* **1985**, *31*, 1695−1697.

(4) Frenkel, D.; Smit, B. *Understanding Molecular Simulation*, 2nd ed.; Academic Press: Orlando, FL, 2002.

(5) Lennard-Jones, J. E. On the Determination of Molecular Fields: I: From the Variation of the Viscosity of a Gas with Temperature. *Proc. R. Soc. London, Ser. A* **1924**, *106*, 441−462.

(6) Jorgensen, W. L.; Chandrasekhar, J.; Madura, J.; Impey, R. W.; Klein, M. L. Comparison of simple potential functions for simulating liquid water. *J. Chem. Phys.* **1983**, *79*, 926−935.

(7) Kristóf, T.; Liszi, J. Effective Intermolecular Potential for Fluid Hydrogen Sulfide. *J. Phys. Chem. B* **1997**, *101*, 5480−5483.

(8) Harris, J. G.; Yung, K. H. Carbon Dioxide's Liquid-Vapor Coexistence Curve And Critical Properties as Predicted by a Simple Molecular Model. *J. Phys. Chem.* **1995**, *99*, 12021−12024.

(9) Jorgensen, W. L.; Madura, J. D.; Swenson, C. J. Optimized Intermolecular Potential Functions for Liquid Hydrocarbons. *J. Am. Chem. Soc.* **1984**, *106*, 6638−6646.

(10) Mezei, M. Polynomial path for the calculation of liquid state free energies from computer simulations tested on liquid water. *J. Comput. Chem.* **1992**, *13*, 651−656.

(11) Cordero, R. R.; Seckmeyer, G.; Pissulla, D.; Labbe, F. Uncertainty of experimental integrals: application to the UV index calculation. *Metrologia* **2008**, *45*, 1−10.

(12) Lyubartsev, A. P.; Laaksonen, A. M. DynaMix−a scalable portable parallel MD simulation package for arbitrary molecular mixtures. *Comput. Phys. Commun.* **2000**, *128*, 565−589.

(13) Førrisdahl, O. K. *Computer simulations of natural gas hydrates: equilibrium, melting, inhibition and free energy calculations*. PhD thesis, Department of Physics, University of Bergen, 2002.

(14) Spycher, N.; Pruess, K.; Ennis-King, E. CO2-H2O mixtures in the geological sequestration of CO2. I. Assessment and calculation of mutual solubilities from 12 to 100 C and up to 600 bar. *Geochim. Cosmochim. Acta* **2003**, *67*, 3015−3031.

(15) Prausnitz, J. M.; Lichtenthaler, R. N.; Gomes de Azevedo, E. *Molecular Thermodynamics of Fluid-Phase Equilibria*, 3rd ed.; Prentice Hall PTR: Upper-Saddle River, NJ, 1999.

(16) Kvamme, B.; Kuznetsova, T.; Kivelæ, P.-H.; Bauman, J. Can hydrate form in carbon dioxide from dissolved water? *Phys. Chem. Chem. Phys.* **2013**, *15*, 2063−2074.

(17) Kvamme, B.; Kuznetsova, T.; Kivelæ, P.-H. Adsorption of water and carbon dioxide on hematite and consequences for possible hydrate formation. *Phys. Chem. Chem. Phys.* **2012**, *14*, 4410−4424.

(18) Kvamme, B.; Tanaka, H. Thermodynamic Stability of Hydrates for Ethane, Ethylene, and Carbon Dioxide. *J. Phys. Chem.* **1995**, *99*, 7114−7119.

Publication Date (Web): September 9, 2015 | doi: 10.1021/acs.jced.5b00267

DOI: 10.1021/acs.jced.5b00267
J. Chem. Eng. Data XXXX, XXX, XXX−XXX